Synthesis, Structures, and Properties of "Encapsulated" Iron and Cobalt Metallocenes with Highly Isopropylated Cyclopentadienyl Rings

David J. Burkey, Melanie L. Hays, Randall E. Duderstadt, and Timothy P. Hanusa*

Department of Chemistry, Vanderbilt University, Nashville, Tennessee 37235

Received August 26, 1996[⊗]

Bis(triisopropylcyclopentadienyl)cobalt, $[(i\text{-Pr})_3C_5H_2]_2Co$, and bis(tetraisopropylcyclopentadienyl)cobalt, $[(i\text{-Pr})_4C_5H]_2Co$, can be prepared from the reaction of $K[(i\text{-Pr})_3C_5H_2]$ and $K[(i\text{-Pr})_4C_5H]$, respectively, with $CoCl_2$ in THF. In contrast to $[(i\text{-Pr})_3C_5H_2]_2Co$, solid samples of the "encapsulated" $[(i\text{-Pr})_4C_5H]_2Co$ are indefinitely stable in air. Bis(triisopropylcyclopentadienyl)iron, $[(i\text{-Pr})_3C_5H_2]_2Fe$, and bis(tetraisopropylcyclopentadienyl)iron, $[(i\text{-Pr})_4C_5H]_2Fe$, can be oxidized with $NOBF_4$ to give the corresponding ferrocenium salts $\{[(i\text{-Pr})_3C_5H_2]_2Fe\}BF_4$ and $\{[(i\text{-Pr})_4C_5H]_2Fe\}BF_4$ in high yield. Oxidation of $[(i\text{-Pr})_3C_5H_2]_2Co$ and $[(i\text{-Pr})_4C_5H]_2Co$ with NH_4X ($X = [PF_6]^-$, $[BPh_4]^-$) yields the cobaltocenium complexes $\{[(i\text{-Pr})_3C_5H_2]_2Co\}X$ and $\{[(i\text{-Pr})_4C_5H]_2Co\}X$. The oxidation of $[(i\text{-Pr})_4C_5H]_2M$ (M = Fe or Co) is significantly slower than that for $[(i\text{-Pr})_3C_5H_2]_2M$. The single-crystal X-ray structures of the neutral $[(i\text{-Pr})_3C_5H_2]_2M$ metallocenes and cationic $\{[(i\text{-Pr})_3C_5H_2]_2M\}^+$ and $\{[(i\text{-Pr})_4C_5H]_2M\}^+$ metallocenes are reported. The structures of the bis(triisopropylcyclopentadienyl)metallocenes are undistorted, with nearly parallel rings and average M-C(ring) distances of 2.05(1) ($[(i\text{-Pr})_3C_5H_2]_2Fe$), 2.08(2)−2.10(2) ($\{[(i\text{-Pr})_3C_5H_2]_2Fe\}BF_4$), 2.122(7) ($[(i\text{-Pr})_3C_5H_2]_2Co$), and 2.05(2) Å ($\{[(i\text{-Pr})_3C_5H_2]_2Co\}BPh_4$). In contrast, $\{[(i\text{-Pr})_4C_5H]_2Fe\}BF_4$ and $\{[(i\text{-Pr})_4C_5H]_2Co\}PF_6$ display sterically induced distortions in the M-C(ring) distances (lengthened to 2.14(2) and 2.09(2) Å) and the inter-ring angles (ring normal-M-ring normal angles of 170.7° and 171.5°), making them the most distorted transition metal metallocenium complexes yet reported. The $\{[(i\text{-Pr})_3C_5H_2]_2Co\}^{0/+}$ and $\{[(i\text{-Pr})_4C_5H]_2Co\}^{0/+}$ redox couples have essentially identical electrochemical potentials, despite the two additional electron-donating isopropyl substituents in the latter complexes. Additionally, oxidation of $[(i\text{-Pr})_4C_5H]_2Fe$ is more favorable than expected for a ferrocene with eight alkyl groups. The anomalous electrochemical data can be attributed to the severe steric crowding that is present in the $\{[(i\text{-Pr})_4C_5H]_2M\}^{0/+}$ complexes.

Introduction

Main-group element metallocenes that differ only in the number of isopropyl substituents on their cyclopentadienyl rings often exhibit strikingly different reactions and physical properties. In general, those constructed from tetraisopropylcyclopentadienyl ligands (i.e., $[(C_3H_7)_4C_5H]_2M$; M = Ca, Sr, Ba, Sn) are crystalline solids that display reduced reactivity toward air and nucleophiles,[1,2] whereas the triisopropylcyclopentadienyl analogues $[(C_3H_7)_3C_5H_2]_2M$ are highly air-sensitive, low-melting solids, oils, or waxes.[2−4] These differences have been linked to structural features of the ligands themselves. In the $[(C_3H_7)_4C_5H]^-$ ligand, the four isopropyl groups are sterically forced to lie nearly perpendicularly to the C_5 ring plane; thus, when two of the ligands are coordinated to a metal, an interlocking cover is formed that protects the metal center from potential reactants and leads to well-ordered crystalline materials. The three isopropyl groups in the $[(C_3H_7)_3C_5H_2]^-$ ligand, in contrast, are less restricted to perpendicular arrangements, reducing any encapsulation of the metal center. The increased conformational flexibility of $[(C_3H_7)_3C_5H_2]^-$ may also make it more difficult to achieve a unique packing arrangement, thereby lowering lattice stabilization and melting temperatures.[4]

Despite these intriguing results in main-group chemistry, no general survey has been made of the effects of these ligands on transition metal metallocenes. Several years ago, Sitzmann reported the synthesis and spectroscopic characterization of the ferrocene derivatives $(Cp^{3i})_2Fe$ ($Cp^{3i} = [(C_3H_7)_3C_5H_2]^-$) and $(Cp^{4i})_2Fe$ ($Cp^{4i} = [(C_3H_7)_4C_5H]^-$),[5] but no structural data or further studies on transition metal metallocenes containing either $[Cp^{3i}]^-$ or $[Cp^{4i}]^-$ ligands have appeared in the literature.[6−8] A detailed examination of such complexes seems warranted, and hence, the synthesis and structural characterization of the iron and cobalt $(Cp^{3i})_2M$

[⊗] Abstract published in *Advance ACS Abstracts,* March 1, 1997.

(1) Williams, R. A.; Tesh, K. F.; Hanusa, T. P. *J. Am. Chem. Soc.* **1991**, *113*, 4843−4851.
(2) Burkey, D. J.; Hanusa, T. P. *Organometallics* **1995**, *14*, 11−13.
(3) Burkey, D. J.; Williams, R. A.; Hanusa, T. P. *Organometallics* **1993**, *12*, 1331−1337.
(4) Burkey, D. J.; Hanusa, T. P.; Huffman, J. C. *Adv. Mater. Opt. Electron.* **1994**, *4*, 1−8.
(5) Sitzmann, H. J. *J. Organomet. Chem.* **1988**, *354*, 203−214.
(6) There have been several recent reports describing mono(cyclopentadienyl) transition metal complexes with $[Cp^{3i}]^-$ and $[Cp^{4i}]^-$ ligands. See refs 7 and 8.
(7) Sitzmann, H.; Zhou, P.; Wolmershäuser, G. *Chem. Ber.* **1994**, *127*, 3−9.
(8) Sitzmann, H.; Wolmershäuser, G. *Z. Naturforsch. B: Anorg. Chem. Org. Chem.* **1995**, *50*, 750−756.

S0276-7333(96)00740-6 CCC: $14.00

and $(Cp^{4i})_2M$ metallocenes and their cations are presented here.

Experimental Section

General Experimental Considerations. Unless otherwise noted, all manipulations were performed with the exclusion of air and moisture using high-vacuum, Schlenk, or drybox techniques. Proton and carbon (^{13}C) NMR spectra were obtained on a Bruker NR-300 spectrometer at 300 MHz and 75.5 MHz, respectively, and were referenced to the residual proton and ^{13}C resonances of C_6D_6 (δ 7.15), acetone-d_6 (δ 2.04 and 29.8), or DMSO-d_6 (δ 2.49). Assignments in the ^{13}C NMR spectra were made with the help of DEPT pulse experiments. Infrared data were obtained on a Perkin-Elmer 1600 Series FT-IR spectrometer. For air-sensitive compounds, KBr pellets for IR spectroscopy were prepared as previously described.[1] Solution magnetic susceptibility data were obtained using Evans' method in C_6D_6 or THF-d_8.[9−12] UV−vis spectra were obtained on a Shimadzu UV-2101PC spectrometer. Elemental analyses were performed by Oneida Research Services, Whitesboro, NY.

Materials. Iron(II) chloride, ammonium hexafluorophosphate, ammonium tetraphenylborate, and nitrosonium tetrafluoroborate were commercial samples (Aldrich or Alfa) and were used as received. Nominally anhydrous cobalt(II) chloride (Aldrich) was heated under vacuum (150 °C, 10^{-6} Torr) to ensure the complete removal of coordinated water. KCp^{3i} and KCp^{4i} were prepared as previously described.[1] $(Cp^{3i})_2Fe$ and $(Cp^{4i})_2Fe$ were prepared by a slight modification of the literature method;[5] i.e., KCp^{3i} and KCp^{4i} were used in place of the sodium salts, and the products were recrystallized from acetone/hexanes at room temperature. The solvents for reactions conducted under anhydrous and anaerobic conditions were distilled under nitrogen from sodium or potassium benzophenone ketyl;[13] otherwise, solvents were reagent grade and used as received. C_6D_6 was vacuum distilled from Na/K (22/78) alloy and stored over 4A molecular sieves prior to use. Acetone-d_6, DMSO-d_6, and $CDCl_3$ were used as received.

Electrochemical Measurements. Single-sweep cyclic voltammetric data were obtained for $(Cp^{3i})_2Fe$, $(Cp^{4i})_2Fe$, $[(Cp^{3i})_2Co]PF_6$, and $[(Cp^{4i})_2Co]PF_6$ in CH_2Cl_2 using an EG & G Princeton Applied Research Potentiostat/Galvanostat Model 273. A four-necked cyclic voltammetry (CV) cell (10 mL) equipped with a Pt disc (1.5 mm diameter) working electrode, a Pt wire counter electrode, and a saturated calomel electrode (SCE) reference electrode was used for CV measurements that were carried out under an inert atmosphere. Tetrabutylammonium tetrafluoroborate (TBABF$_4$, Kodak) was used as the supporting electrolyte (0.1 M solution).

Synthesis of $(Cp^{3i})_2Co$. A suspension of KCp^{3i} (0.78 g, 3.39 mmol) in 30 mL of THF was cooled to −78 °C in a dry ice/acetone bath. Over the course of 10 min, 50 mL of a THF solution of $CoCl_2$ (0.20 g, 1.50 mmol) was added from a dropping funnel; during this time, the reaction mixture turned dark green and then black. The reaction was stirred at −78 °C for 1 h; the dry ice/acetone bath was then removed, and the reaction was stirred an additional 18 h, while it warmed to room temperature. The THF was removed under vacuum, and the black residue was extracted with 50 mL of hexanes and filtered through a glass frit to remove a bluish precipitate. Removal of the hexanes under vacuum and fractional sublimation of the remaining black solid (60−110 °C, 10^{-6} Torr) gave 0.42 g (63% yield) of $(Cp^{3i})_2Co$ as a brown powder (mp 136−138 °C). Anal. Calcd for $C_{28}H_{46}Co$: C, 76.16; H, 10.50; Co, 13.35. Found: C, 76.07; H, 10.36; Co, 13.12. ^1H NMR (C_6D_6): δ 7.98 ($\omega_{1/2}$ = 28 Hz), 6.96 ($\omega_{1/2}$ = 82 Hz), 2.78 ($\omega_{1/2}$ = 20 Hz), 1.93 ($\omega_{1/2}$ = 30 Hz); the relative intensities of the resonances are ca. 3:1:6:3. μ_{corr} (297 K): 2.02 μ_B. Principal IR bands (KBr, cm^{-1}): 2951 (s), 2934 (sh), 1460 (s), 1410 (w), 1384 (m), 1363 (m), 1276 (w), 1178 (m), 1104 (s), 1040 (w), 880 (w), 660 (m), 641 (w), 561 (w), 457 (w). Solid samples of $(Cp^{3i})_2Co$ exposed to air decompose over the course of a few minutes, leaving a black sticky residue.

Synthesis of $(Cp^{4i})_2Co$. Using the procedure described for $(Cp^{3i})_2Co$, the reaction of KCp^{4i} (0.67 g, 2.46 mmol) and $CoCl_2$ (0.15 g, 1.15 mmol) yielded, after fractional sublimation at 140−150 °C and 10^{-6} Torr, 0.32 g (53% yield) of $(Cp^{4i})_2Co$ as a dark brown powder (mp 148−150 °C). Anal. Calcd for $C_{34}H_{58}Co$: C, 77.67; H, 11.12. Found: C, 77.88; H, 10.87. ^1H NMR (C_6D_6): δ 11.3 ($\omega_{1/2}$ = 390 Hz), 8.0 ($\omega_{1/2}$ = 300 Hz), 6.5 ($\omega_{1/2}$ = 115 Hz), 4.2 ($\omega_{1/2}$ = 210 Hz), 1.6 ($\omega_{1/2}$ = 150 Hz). μ_{corr} (297 K): 1.97 μ_B. Principal IR bands (KBr, cm^{-1}): 2966 (s), 2930 (sh), 2871 (sh), 1457 (m), 1378 (m), 1359 (m), 1294 (w), 1178 (m), 1146 (m), 1101 (m), 1057 (w), 1044 (w), 824 (w), 657 (w), 645 (w), 609 (w), 460 (w). In the solid state, $(Cp^{4i})_2Co$ is stable for over 6 months in air; in contrast, solutions of $(Cp^{4i})_2Co$ decompose within several minutes on exposure to oxygen.

Synthesis of $[(Cp^{3i})_2Fe]BF_4$. In air, $(Cp^{3i})_2Fe$ (0.29 g, 0.66 mmol) was dissolved in 20 mL of CH_2Cl_2 (dried over 4A molecular sieves prior to use) in a 50 mL three-neck flask. The flask was then fitted with two stoppers and a gas inlet and connected to a Schlenk line; the air in the flask was removed by two freeze−pump−thaw cycles and replaced with an atmosphere of N_2. To the stirred $(Cp^{3i})_2Fe$ solution was added solid $NOBF_4$ (0.12 g, 1.0 mmol, preweighed under N_2) against a stream of N_2; the color of the reaction changed from orange to a dark green-black almost immediately. The reaction was stirred for 1 h under nitrogen and then opened to air and filtered through a glass frit to remove unreacted $NOBF_4$. The dark green filtrate was concentrated to a volume of 5 mL by rotary evaporation and then layered with 15 mL of Et_2O and stored at −20 °C. After a few hours, the solid that had precipitated was separated from the CH_2Cl_2/Et_2O by decantation, washed twice with 10 mL of Et_2O, and dried briefly under vacuum to give 0.29 g (84% yield) of $[(Cp^{3i})_2Fe]BF_4$ as an air-stable, deep forest-green powder (mp > 250 °C). Anal. Calcd for $C_{28}H_{46}BF_4Fe$: C, 64.02; H, 8.83; Fe, 10.63. Found: C, 63.79; H, 8.81; Fe, 10.83. ^1H NMR (acetone-d_6): δ 13.5 ($\omega_{1/2}$ = 150 Hz), −6.2 ($\omega_{1/2}$ = 220 Hz), −14.5 ($\omega_{1/2}$ = 440 Hz), −30.6 ($\omega_{1/2}$ = 250 Hz); the relative intensities of the resonances are ca. 5:5:1:5. μ_{corr} (297 K): 2.68 μ_B. Principal IR bands (KBr, cm^{-1}): 3096 (w), 2973 (s, br), 2934 (sh), 2875 (sh), 1488 (m), 1464 (m), 1431 (w), 1386 (m), 1367 (m), 1328 (w), 1282 (w), 1265 (m), 1182 (w), 1155 (w), 1092 (s), 1052 (s, br, B-F), 926 (w), 909 (w), 875 (w), 803 (w), 725 (w), 642 (w), 592 (w), 520 (w), 456 (w). UV−vis (THF, λ in nm; ϵ in L mol^{-1} cm^{-1}): λ_{max} 221 (13 400, shoulder), 280 (15 000), 317 (11 100), 600 (490).

Synthesis of $[(Cp^{4i})_2Fe]BF_4$. The procedure described for the synthesis of $[(Cp^{3i})_2Fe]BF_4$ was repeated, using $(Cp^{4i})_2Fe$ (0.30 g, 0.57 mmol) and $NOBF_4$ (0.14 g, 1.17 mmol) in CH_2Cl_2; however, the reaction was allowed to stir for 12 h. After workup, 0.31 g (89% yield) of $[(Cp^{4i})_2Fe]BF_4$ was isolated as an air-stable, deep forest-green powder (mp > 250 °C). Anal. Calcd for $C_{34}H_{58}BF_4Fe$: C, 67.00; H, 9.59; Fe, 9.16. Found: C, 66.37; H, 9.42; Fe, 9.49. ^1H NMR (acetone-d_6): δ 15.0 ($\omega_{1/2}$ = 270 Hz), 12.3 (shoulder), 10.6 ($\omega_{1/2}$ = 575 Hz), −11.0 ($\omega_{1/2}$ = 900 Hz), −22.0 (shoulder), −24.4 ($\omega_{1/2}$ = 1050 Hz), −30.5 ($\omega_{1/2}$ = 420 Hz). μ_{corr}: 2.27 μ_B. Principal IR bands (KBr, cm^{-1}): 3105 (w), 2976 (s), 2938 (sh), 2880 (sh), 1465 (s), 1402 (w), 1381 (m), 1368 (m), 1317 (w), 1264 (w), 1192 (w), 1151 (m), 1087 (s), 1058 (s, B-F), 968 (m), 931 (w), 883 (w), 759 (w), 676 (w), 592 (w), 520 (w), 456 (w). UV−vis (THF, λ in nm; ϵ in L mol^{-1} cm^{-1}): λ_{max} 221 (13 700, shoulder), 295 (15 500), 337 (11 800), 643 (440).

Synthesis of $[(Cp^{3i})_2Co]PF_6$. In a drybox, $(Cp^{3i})_2Co$ (0.23 g, 0.52 mmol) was dissolved in 20 mL of THF in an Erlenmeyer

(9) Evans, D. F. *J. Am. Chem. Soc.* **1959**, *92*, 2003−2005.
(10) Grant, D. H. *J. Chem. Educ.* **1995**, *72*, 39−40.
(11) Sur, S. K. *J. Magn. Reson.* **1989**, *82*, 169−173.
(12) Shubert, E. M. *J. Chem. Educ.* **1992**, *69*, 62.
(13) Perrin, D. D.; Armarego, W. L. F. *Purification of Laboratory Chemicals*, 3rd ed.; Pergamon: Oxford, 1988.

flask; to this was added NH_4PF_6 (90 mg, 0.55 mmol) in small portions. The dark brown reaction mixture was stirred for 8 h, during which time it slowly turned yellow. The reaction mixture was concentrated under vacuum to a volume of 5 mL, and hexanes (15 mL) was added, which led to the formation of a yellow precipitate. This solid was collected by filtration in air, washed twice with hexanes (20 mL), and then twice with H_2O (15 mL). The solid was then dissolved in 10 mL of acetone; centrifugation of the solution removed a small amount of black material. Evaporation of the acetone under vacuum and recrystallization of the residue from acetone/Et_2O (5:1) at −20 °C gave 0.22 g (81% yield) of $[(Cp^{3i})_2Co]PF_6$ as a bright yellow, microcrystalline solid. When heated to 250 °C, $[(Cp^{3i})_2Co]PF_6$ darkens to an orange color, but does not melt. ^{1}H NMR (acetone-d_6): δ 5.63 (s, 4 H, ring-C*H*), 2.78−2.88 (two overlapping septets, 6 H, C*H*Me$_2$), 1.45 (d, J = 6.7 Hz, 12 H, C*H*$_3$), 1.25 (d, J = 6.9 Hz, 12 H, C*H*$_3$), 1.13 (d, J = 6.6 Hz, 12 H, C*H*$_3$). ^{13}C NMR (acetone-d_6): δ 111.3 (ring-*C*CHMe$_2$), 78.1 (ring-*C*H), 27.4 (*C*HMe$_2$), 25.5 (*C*HMe$_2$), 25.3 (*C*H$_3$), 23.1 (*C*H$_3$), 22.7 (*C*H$_3$). Principal IR bands (KBr, cm^{-1}): 3115 (w), 2974 (s), 2875 (sh), 1488 (s), 1402 (sh), 1388 (m), 1367 (m), 1321 (w), 1268 (m), 1199 (w), 1181 (w), 1154 (w), 1129 (w), 1101 (w), 1062 (m), 1014 (m), 927 (m), 912 (m), 836 (s, br, P-F), 726 (w), 558 (s), 481 (w).

Synthesis of $[(Cp^{3i})_2Co]BPh_4$. $(Cp^{3i})_2Co$ (0.15 g, 0.34 mmol) was dissolved in 20 mL of THF in an Erlenmeyer flask; to this was added NH_4BPh_4 (0.13 g, 0.39 mmol) in small portions. After 8 h, the now yellow reaction mixture was concentrated (5 mL) and a yellow solid was precipitated by the addition of hexanes (15 mL). The precipitate was collected by filtration in air, washed twice with 5 mL of hexanes, extracted into chloroform (15 mL), and filtered to remove excess NH_4BPh_4. The chloroform was removed under vacuum, and the residue was dissolved in 10 mL of acetone. The solution was then centrifuged to remove a small amount of black material. The acetone solution was subsequently concentrated to a volume of 2 mL and carefully layered with 5 mL of Et_2O. After 24 h at −20 °C, golden yellow crystals of $[(Cp^{3i})_2Co]BPh_4$ (mp 200−212 °C) precipitated from solution; decantation of the remaining solution followed by drying the crystals briefly under vacuum yielded 0.24 g (90% yield) of product. Anal. Calcd for $C_{52}H_{66}BCo$: C, 82.09; H, 8.74; Co, 7.75. Found: C, 81.72; H, 8.51; Co, 7.51. ^{1}H NMR (acetone-d_6): δ 7.33 (br m, 8 H, *o*-Ph), 6.92 (m, 8 H, *m*-Ph), 6.77 (m, 4 H, *p*-Ph), 5.65 (s, 4 H, ring-C*H*), 2.76−2.90 (two overlapping septets, 6 H, C*H*Me$_2$), 1.47 (d, J = 6.6 Hz, 12 H, C*H*$_3$), 1.27 (d, J = 6.8 Hz, 12 H, C*H*$_3$), 1.15 (d, J = 6.6 Hz, 12 H, C*H*$_3$). ^{13}C NMR (acetone-d_6): δ 164.9 (q, ^1J(B-C) = 49.4 Hz, B-*C*(Ph)), 137.0 (*m*-Ph), 125.9 (q, ^2J(B-C) = 2.6 Hz, *o*-Ph), 122.2 (*p*-Ph), 111.3 (ring-*C*CHMe$_2$), 78.1 (ring-*C*H), 27.4 (*C*HMe$_2$), 25.5 (*C*HMe$_2$), 25.3 (*C*H$_3$), 23.1 (*C*H$_3$), 22.7 (*C*H$_3$). Principal IR bands (KBr, cm^{-1}): 3052 (s), 2976 (s), 2875 (sh), 1581 (m), 1480 (s), 1460 (s), 1427 (s), 1383 (m), 1366 (m), 1267 (m), 1182 (m), 1151 (m), 1126 (w), 1054 (m), 1032 (m), 1015 (w), 937 (w), 926 (w), 900 (m), 849 (m), 743 (s), 732 (s), 704 (s), 626 (w), 605 (s), 481 (w), 465 (w).

Synthesis of $[(Cp^{4i})_2Co]PF_6$. $(Cp^{4i})_2Co$ (0.10 g, 0.19 mmol) was dissolved in 10 mL of THF in an Erlenmeyer flask; to this was added NH_4PF_6 (55 mg, 0.34 mmol) in small portions. The dark brown reaction mixture was then stirred for 24 h, during which time it slowly turned yellow. Workup of the reaction following the same procedure used for $[(Cp^{3i})_2Co]PF_6$ gave 0.10 g (79% yield) of $[(Cp^{4i})_2Co]PF_6$ as amber crystals. When heated to 250 °C, $[(Cp^{4i})_2Co]PF_6$ darkens to an orange color, but does not melt. Anal. Calcd for $C_{34}H_{58}CoF_6P$: C, 60.86; H, 8.72; Co, 8.79. Found: C, 60.03; H, 8.70; Co, 8.63. ^{1}H NMR (acetone-d_6): δ 5.65 (s, 2 H, ring-C*H*), 3.09 (septet, J = 6.8 Hz, 8 H, C*H*Me$_2$), 1.60 (br, 12 H, CH$_3$), 1.47 (br d, 12 H, C*H*$_3$), 1.42 (br, 12 H, C*H*$_3$), 1.16 (br d, 12 H, C*H*$_3$). ^{13}C NMR (acetone-d_6): δ 111.5 (vbr, ring-*C*CHMe$_2$), 108.0 (vbr, ring-*C*CHMe$_2$), 74.0 (br, ring-*C*H), 27.2 (br, *C*HMe$_2$), 27.0 (*C*HMe$_2$), 26.8 (*C*H$_3$), 24.5 (br, *C*H$_3$), 23.9 (br, *C*H$_3$), 22.0 (br, *C*H$_3$). Principal IR bands (KBr, cm^{-1}): 3130 (w), 2979 (s, br), 2881 (sh), 1461 (s, br), 1402 (s), 1386 (s), 1368 (s), 1338 (m), 1316 (m), 1296 (m), 1266 (m), 1194 (m), 1169 (w), 1150 (w), 1102 (m), 1085 (m), 1069 (m), 1057 (m), 1034 (w), 972 (w), 934 (w), 898 (sh), 846 (s, br, P-F), 760 (w), 739 (w), 681 (w), 558 (s), 480 (w).

Synthesis of $[(Cp^{4i})_2Co]BPh_4$. $(Cp^{4i})_2Co$ (0.12 g, 0.22 mmol) was dissolved in 15 mL of THF in an Erlenmeyer flask; to this was added NH_4BPh_4 (85 mg, 0.25 mmol) in small portions. The dark brown reaction mixture was then stirred for 24 h, during which time it slowly turned yellow. Workup of the reaction following the same procedure used for $[(Cp^{3i})_2Co]BPh_4$ gave 0.14 g (77% yield) of $[(Cp^{4i})_2Co]BPh_4$ as an orange-yellow, microcrystalline solid (mp 200−215 °C). Anal. Calcd for $C_{58}H_{78}BCo$: C, 82.44; H, 9.30; Co, 6.97. Found: C, 82.33; H, 9.48; Co, 7.04. ^{1}H NMR (DMSO-d_6, 60 °C): δ 7.17 (br m, 8 H, *o*-Ph), 6.90 (t, J = 7.2 Hz, 8 H, *m*-Ph), 6.76 (t, J = 7.1 Hz, 4 H, *p*-Ph), 5.53 (s, 2 H, ring-C*H*), 2.92 (septet, J = 6.9 Hz, 8 H, C*H*Me$_2$), 1.47 (d, J = 7.0 Hz, 12 H, C*H*$_3$), 1.37 (d, J = 6.6 Hz, 12 H, C*H*$_3$), 1.29 (d, J = 6.9 Hz, 12 H, C*H*$_3$), 1.06 (d, J = 6.5 Hz, 12 H, C*H*$_3$). ^{1}H NMR (acetone-d_6): δ 7.34 (br m, 8 H, *o*-Ph), 6.92 (t, J = 7.3 Hz, 8 H, *m*-Ph), 6.78 (t, J = 7.1 Hz, 4 H, *p*-Ph), 5.63 (s, 2 H, ring-C*H*), 3.07 (septet, J = 6.9 Hz, 8 H, C*H*Me$_2$), 1.58 (br d, 12 H, C*H*$_3$), 1.46 (br d, 12 H, C*H*$_3$), 1.40 (br d, 12 H, C*H*$_3$), 1.15 (d, J = 6.6 Hz, 12 H, C*H*$_3$). ^{13}C NMR (acetone-d_6): δ 164.9 (q, ^1J(B-C) = 49.5 Hz, B-*C*(Ph)), 137.0 (*m*-Ph), 125.90 (q, ^2J(B-C) = 2.6 Hz, *o*-Ph), 122.1 (*p*-Ph), 111.4 (vbr, ring-*C*CHMe$_2$), 108.0 (vbr, ring-*C*CHMe$_2$), 7.40 (br, ring-*C*H), 27.2 (br, *C*HMe$_2$), 26.9 (*C*HMe$_2$), 26.8 (*C*H$_3$), 24.6 (br, *C*H$_3$), 23.9 (br, *C*H$_3$), 22.0 (br, *C*H$_3$). Principal IR bands (KBr, cm^{-1}): 3055 (s), 2999 (s), 2982 (sh), 2879 (sh), 1579 (m), 1479 (s), 1458 (s), 1426 (w), 1385 (m), 1367 (m), 1311 (w), 1264 (w), 1232 (w), 1185 (m), 1153 (m), 1086 (w), 1062 (w), 1052 (w), 1032 (m), 972 (w), 883 (w), 845 (w), 744 (s), 733 (s), 705 (s), 624 (w), 613 (s), 602 (m), 534 (w), 490 (w), 465 (w).

General Procedures for X-ray Crystallography. A suitable crystal of each compound was located and either sealed in a glass capillary (for $(Cp^{3i})_2Co$) or mounted on a glass fiber in air. All measurements were performed at 20 °C on a Rigaku AFC6S diffractometer at Vanderbilt University with graphite-monochromated Mo Kα (λ = 0.710 69 Å) or Cu Kα radiation (λ = 1.541 78 Å). Relevant crystal and data collection parameters for the compounds are given in Table 1.

Cell constants and orientation matrices for data collection were obtained from systematic searches of limited hemispheres of reciprocal space; sets of diffraction maxima were located whose setting angles were refined by least squares. The space groups were determined from consideration of the unit cell parameters, statistical analyses of intensity distributions, and, where appropriate, systematic absences. Subsequent solution and refinement of the structures confirmed the choice in each case.

Data collection was performed using continuous $\omega-2\theta$ scans with stationary backgrounds (peak/background counting time = 2:1). Data were reduced to a unique set of intensities and associated σ values in the usual manner. The structures were solved by direct methods (SHELXS-86, DIRDIF) and Fourier techniques and refined using the full-matrix, least-squares method of TEXSAN.[14] All non-hydrogen atoms were refined anisotropically, except when prohibited by a low number of observed reflections. Except as noted below, hydrogen atoms were inserted in calculated positions based on packing considerations and d(C-H) = 0.95 Å; the positions were fixed for the final cycles of refinement. Final difference maps were featureless. Special considerations given to the individual structures are detailed below.

$(Cp^{3i})_2Fe$. Only needlelike crystals of $(Cp^{3i})_2Fe$ could be grown from any solvent; the most regular in shape were obtained from acetone. The iron atom in the metallocene was located on an inversion center. Although the absorption

(14) *TEXSAN. TEXRAY Structure Analysis Package.* TEXSAN Molecular Structure Corporation: The Woodlands, TX, 1985.

Table 1. Crystal Data and Summary of X-ray Data Collection

	$(Cp^{3i})_2Fe$	$[(Cp^{3i})_2Fe]BF_4$	$[(Cp^{4i})_2Fe]BF_4$	$(Cp^{3i})_2Co$	$[(Cp^{3i})_2Co]BPh_4$	$[(Cp^{4i})_2Co]PF_6$
formula	$C_{28}H_{46}Fe$	$C_{28}H_{46}BF_4Fe$	$C_{34}H_{58}BF_4Fe$	$C_{28}H_{46}Co$	$C_{52}H_{66}BCo$	$C_{34}H_{58}CoF_6P$
fw	438.52	525.32	609.48	441.61	760.84	670.73
color of cryst	orange	green-black	forest green	brown	yellow	amber
cryst dimens, mm	0.085 × 0.20 × 0.44	0.28 × 0.40 × 0.58	0.05 × 0.38 × 0.73	0.26 × 0.30 × 0.88	0.23 × 0.35 × 0.56	0.55 × 0.50 × 0.13
space group	$P\bar{1}$	$P\bar{1}$	*Pbca*	$P\bar{1}$	$I\bar{4}2d$	*Pbca*
a, Å	9.063(4)	10.218(3)	19.12(1)	9.103(3)	16.837(4)	19.384(4)
b, Å	9.333(3)	14.906(4)	21.707(6)	9.359(5)		22.095(4)
c, Å	8.810(4)	9.613(2)	16.304(6)	8.850(3)	30.810(7)	16.346(5)
α, deg	101.12(3)	101.12(3)		101.03(4)		
β, deg	118.38(3)	100.55(2)		118.44(2)		
γ, deg	76.13(3)	84.06(2)		77.08(4)		
V, Å^3	633.8(5)	1427(1)	6767(6)	643.0(5)	8734(4)	7001(3)
Z	1	2	8	1	8	8
D(calcd), g/cm^3	1.149	1.222	1.19	1.140	1.157	1.27
radiation type	Mo Kα	Cu Kα	Mo Kα	Cu Kα	Mo Kα	Mo Kα
abs coeff, cm^{-1}	6.04	45.78	4.85	55.24	4.23	5.85
transmn factors	0.77−1.40	0.45−1.41	0.64−1.00	0.91−1.00	no correction	no correction
scan speed, deg/min	2.0	4.0	2.0	4.0	4.0	4.0
scan width	1.15 + 0.30 tan θ	1.57 + 0.30 tan θ	0.94 + 0.30 tan θ	1.37 + 0.30 tan θ	1.31 + 0.30 tan θ	0.94 + 0.30 tan θ
limits of data collcn, deg	$6 \le 2\theta \le 50$	$20 \le 2\theta \le 120$	$6 \le 2\theta \le 45$	$6 \le 2\theta \le 120$	$6 \le 2\theta \le 50$	$6 \le 2\theta \le 50$
total no. reflns	2394	4514	4919	2042	2229	6817
no. unique reflns	2240	4240	4919	1902	2229	6817
no. with $I > 3.0\sigma(I)$	1275	1695	1460	1471	968	2655
R(*F*)	0.061	0.080	0.065	0.036	0.049	0.050
$R_w(F)$	0.075	0.090	0.074	0.042	0.055	0.056
goodness of fit	2.05	2.67	1.89	1.43	1.76	1.56
max Δ/σ in final cycle	0.02	0.07	0.18	0.12	0.04	0.01
max/min peak (final diff map) (e$^-$/Å^3)	0.49/−0.63	0.59/−0.40	0.45/−0.35	0.19/−0.17	0.42/−0.24	0.60/−0.41

Table 2. Selected Bond Distances (Å) and Angles (deg) for $(Cp^{3i})_2Fe$

Fe(1)−C(2)	2.066(6)	C(2)−C(3)	1.435(9)
Fe(1)−C(3)	2.049(7)	C(2)−C(6)	1.406(9)
Fe(1)−C(4)	2.050(6)	C(3)−C(4)	1.422(9)
Fe(1)−C(5)	2.067(6)	C(4)−C(5)	1.429(9)
Fe(1)−C(6)	2.044(6)	C(5)−C(6)	1.411(9)
Fe(1)−ring centroid	1.662(7)	C(ring)−CH (av)	1.51(2)

CH_3−CH−CH_3 (av)	109(1)
ring centroid−Fe(1)−ring centroid	180
ring normal−Fe(1)−ring normal	180
av displacement of methine carbon from ring plane	0.12
planarity of ring	within 0.013

Table 3. Selected Bond Distances (Å) and Angles (deg) for $(Cp^{3i})_2Co$

Co(1)−C(2)	2.140(3)	C(2)−C(3)	1.414(4)
Co(1)−C(3)	2.116(3)	C(2)−C(6)	1.423(5)
Co(1)−C(4)	2.111(3)	C(3)−C(4)	1.407(5)
Co(1)−C(5)	2.115(3)	C(4)−C(5)	1.438(4)
Co(1)−C(6)	2.128(3)	C(5)−C(6)	1.415(5)
Co(1)−ring centroid	1.745(3)	C(ring)−CH (av)	1.505(9)

CH_3−CH−CH_3(av)	110.4(8)
ring centroid−Co(1)−ring centroid	180
ring normal−Co(1)−ring normal	180
av displacement of methine carbon from ring plane	0.081
planarity of ring	within 0.010

coefficient was relatively low, the large differences in crystal dimensions necessitated an absorption correction; this was done semiempirically using the program DIFABS. Selected bond distances and angles are listed in Table 2.

$(Cp^{3i})_2Co$. Crystals of $(Cp^{3i})_2Co$ were grown from toluene. An absorption correction based on ψ-scans of suitable reflections was applied. The molecule is isostructural with $(Cp^{3i})_2Fe$. All of the hydrogen atoms were clearly visible in difference Fourier maps, and their positions were allowed to refine isotropically. Selected bond distances and angles are listed in Table 3.

$[(Cp^{3i})_2Fe]BF_4$. Single crystals of $[(Cp^{3i})_2Fe]BF_4$ were grown from acetone/water as thin plates. An absorption correction based on ψ-scans of suitable reflections was applied. Two separate locations were identified for the iron atoms on special positions; the metallocene cations associated with each iron were essentially identical. The fluorine atoms of the $[BF_4]^-$ anion exhibited high thermal parameters ($B_{iso} \ge 19$ Å^2), possibly owing to a slight disorder that could not be resolved. Selected bond distances and angles are listed in Table 4.

Table 4. Selected Bond Distances (Å) and Angles (deg) for $[(Cp^{3i})_2Fe]BF_4$

Fe(1)−C(2)	2.09(1)	Fe(2)−C(2A)	2.13(1)
Fe(1)−C(3)	2.07(1)	Fe(2)−C(3A)	2.04(1)
Fe(1)−C(4)	2.10(1)	Fe(2)−C(4A)	2.09(1)
Fe(1)−C(5)	2.09(1)	Fe(2)−C(5A)	2.13(1)
Fe(1)−C(6)	2.07(1)	Fe(2)−C(6A)	2.10(1)
Fe(1)−ring centroid	1.71(1)	Fe(2)−ring centroid	1.71(1)
C(2)−C(3)	1.38(2)	C(2A)−C(3A)	1.41(2)
C(2)−C(6)	1.39(2)	C(2A)−C(6A)	1.42(2)
C(3)−C(4)	1.41(2)	C(3A)−C(4A)	1.42(2)
C(4)−C(5)	1.44(2)	C(4A)−C(5A)	1.42(2)
C(5)−C(6)	1.40(2)	C(5A)−C(6A)	1.46(2)
C(ring)−CH (av)	1.53(3)	C(ring)−CH (av)	1.53(3)
CH−CH_3 (av)	1.51(4)	CH−CH_3 (av)	1.54(4)

CH_3−CH−CH_3 (av)	109(2)
CH_3−CH−CH_3 (av)	110(2)
ring centroid−Fe(1,2)−ring centroid	180, 180
planarity of Fe(1) ring	within 0.002
ring normal−Fe(1,2)−ring normal	180, 180
planarity of Fe(2) ring	within 0.02
av displacement of methine carbons from ring plane	0.13, 0.10

$[(Cp^{3i})_2Co]BPh_4$. Well-shaped yellow blocks of $[(Cp^{3i})_2Co]BPh_4$ were grown from acetone. Although statistics suggested a centrosymmetric space group for the tetragonal unit cell, the systematic absences (*hkl*; $h + k + l \neq 2n$; *hhl*; $2h + 1 \neq 4n$) were consistent only with the acentric groups $I4_1md$ (No. 109) and $I\bar{4}2d$ (No. 122). The latter was chosen as being more consistent with the probable symmetry of the molecule; subsequent solution and refinement of the structure confirmed this choice. No decay was evident in the intensities of three representative reflections measured after every 150 reflections. The cobalt atom of the metallocene was located on a 2-fold axis. There were two positions for the tetraphenylborate anion, each at half-occupancy relative to the metallocene; the boron atoms were located on $\bar{4}$ sites. The lack of a sufficient number of observed reflections meant that not all atoms could be refined anisotropically; the carbon atom positions of the tetraphenylborate anions were determined with isotropic thermal param-

Table 5. Selected Bond Distances (Å) and Angles (deg) for $[(Cp^{3i})_2Co]BPh_4$

Co(1)−C(2)	2.053(9)	C(2)−C(3)	1.40(1)
Co(1)−C(3)	2.02(1)	C(2)−C(6)	1.45(1)
Co(1)−C(4)	2.04(1)	C(3)−C(4)	1.46(2)
Co(1)−C(5)	2.08(1)	C(4)−C(5)	1.39(1)
Co(1)−C(6)	2.05(1)	C(5)−C(6)	1.40(1)
Co(1)−ring centroid	1.65(1)	C(16)−B(1)	1.64(1)
C(ring)-CH (av)	1.50(2)	C(27)−B(2)	1.63(1)
CH−CH_3 (av)	1.53(5)	C−C(Ph rings) (av)	1.38(6)

CH_3−CH−CH_3 (av)	110(2)
ring centroid−Co(1)−ring centroid	177.9(7)
ring normal−Co(1)−ring normal	174.7
av displacement of methine carbon from ring plane	0.15
planarity of Cp ring	within 0.004

Table 6. Selected Bond Distances (Å) and Angles (deg) for $[(Cp^{4i})_2Fe]BF_4$

Fe(1)−C(1)	2.10(1)	Fe(1)−C(18)	2.10(1)
Fe(1)−C(2)	2.14(1)	Fe(1)−C(19)	2.18(1)
Fe(1)−C(3)	2.18(1)	Fe(1)−C(20)	2.13(2)
Fe(1)−C(4)	2.18(1)	Fe(1)−C(21)	2.13(2)
Fe(1)−C(5)	2.13(1)	Fe(1)−C(22)	2.14(1)
Fe(1)−ring centroid	1.78(1)	Fe(1)−ring centroid	1.77(2)
C(1)−C(2)	1.40(2)	C(18)−C(19)	1.38(2)
C(1)−C(5)	1.43(2)	C(18)−C(22)	1.38(2)
C(2)−C(3)	1.43(2)	C(19)−C(20)	1.36(2)
C(3)−C(4)	1.40(2)	C(20)−C(21)	1.45(2)
C(4)−C(5)	1.41(2)	C(21)−C(22)	1.44(2)
C(ring)−CH (av)	1.51(6)	CH−CH_3 (av)	1.55(8)

CH_3−CH−CH_3 (av)	110(3)
ring centroid−Fe(1)−ring centroid	174.3(6)
ring normal−Fe(1)−ring normal	170.7
av displacement of methine carbon from ring plane	0.23
planarity of rings	within 0.026

eters in the least-squares refinement. Selected bond distances and angles are listed in Table 5.

$[(Cp^{4i})_2Fe]BF_4$. Single crystals of $[(Cp^{4i})_2Fe]BF_4$ were grown from acetone as thin plates. Owing to the large differences in crystal dimensions, an absorption correction based on ψ-scans of suitable reflections was applied. The crystal was weakly diffracting, and the large number of atoms combined with the lack of reflections meant that not all atoms could be refined anisotropically. The ring and methine carbons of the $[Cp^{4i}]^-$ rings were determined with isotropic thermal parameters in the least-squares refinement. The fluorine atoms of the $[BF_4]^-$ anion exhibited high thermal parameters ($B_{iso} \geq 15$ Å^2), possibly owing to unresolvable disorder. Selected bond distances and angles are listed in Table 6.

$[(Cp^{4i})_2Co]PF_6$. Amber crystals of $[(Cp^{4i})_2Co]PF_6$ grown from acetone were used for data collection. The intensities of three representative reflections, which were measured after every 150 reflections, declined by 4% during data collection; a linear correction factor was applied to the data to account for the decay. Four equatorial fluorine atoms of the $[PF_6]^-$ anion displayed high thermal parameters ($B_{iso} \geq 13$ Å^2) that were indicative of disorder. Consistent with this, the four highest peaks in the final difference map were found to bisect the F-P-F angles for these fluorine atoms. However, the electron density of these positions was very small (<0.6 e$^-$/Å^3), and no attempt was made to model the disorder by partial occupancy of the fluorines at the alternate positions. Selected bond distances and angles are listed in Table 7.

Results

Synthesis of $(Cp^{3i})_2Co$ and $(Cp^{4i})_2Co$. Like the corresponding iron metallocenes,[5] the cobaltocene complexes $(Cp^{3i})_2Co$ and $(Cp^{4i})_2Co$ were synthesized by the metathetical reaction of 2 equiv of either KCp^{3i} or KCp^{4i} with the appropriate metal dichloride in THF (eq 1). The reactions were initiated at low temperature (−78 °C),

Table 7. Selected Bond Distances (Å) and Angles (deg) for $[(Cp^{4i})_2Co]PF_6$

Co(1)−C(1)	2.033(6)	Co(1)−C(18)	2.048(6)
Co(1)−C(2)	2.087(6)	Co(1)−C(19)	2.094(6)
Co(1)−C(3)	2.116(6)	Co(1)−C(20)	2.085(6)
Co(1)−C(4)	2.138(6)	Co(1)−C(21)	2.108(6)
Co(1)−C(5)	2.089(6)	Co(1)−C(22)	2.102(6)
Co(1)−ring centroid	1.706	Co(1)−ring centroid	1.703
C(1)−C(2)	1.410(8)	C(18)−C(19)	1.406(8)
C(1)−C(5)	1.414(8)	C(18)−C(22)	1.392(8)
C(2)−C(3)	1.434(8)	C(19)−C(20)	1.429(8)
C(3)−C(4)	1.431(8)	C(20)−C(21)	1.443(8)
C(4)−C(5)	1.433(8)	C(21)−C(22)	1.429(8)
C(ring)-CH (av)	1.52(2)	CH−CH_3 (av)	1.53(4)

CH_3−CH−CH_3 (av)	109(2)
ring centroid−Co(1)−ring centroid	174.8(3)
ring normal−Co(1)−ring normal	171.5
av displacement of methine carbon from ring plane	0.25
planarity of Cp rings	within 0.025

$$2KCp^{ni} + CoCl_2 \xrightarrow[n = 3,4]{\text{THF, } -78\ ^\circ\text{C}} (Cp^{ni})_2Co + 2KCl\downarrow \quad (1)$$

as substantial decomposition occurred if they were attempted entirely at room temperature.[15,16] Fractional sublimation of the crude products gave both $(Cp^{3i})_2Co$ (mp = 136−138 °C) and $(Cp^{4i})_2Co$ (mp = 148−150 °C) as dark brown powders in good yield (>50%); crystalline samples of the compounds were black.

The paramagnetic cobaltocenes were characterized by elemental analysis, IR spectroscopy, and magnetic susceptibility measurements. The room temperature magnetic moments for $(Cp^{3i})_2Co$ and $(Cp^{4i})_2Co$ (measured by the Evans' method[9−12] in $CDCl_3$) were 2.02 and 1.97 μ_B, respectively, somewhat higher than the values previously found for other neutral cobaltocenes (cf. 1.56 μ_B for Cp^*_2Co and 1.76 μ_B for Cp_2Co[17]), but still indicative of low-spin complexes with one unpaired electron. The identity of the cobaltocenes was also confirmed by their subsequent high-yield conversion to the cobaltocenium salts $[(Cp^{3i})_2Co]X$ and $[(Cp^{4i})_2Co]X$ (X = PF_6 and BPh_4) described below.

When exposed to oxygen, solid $(Cp^{3i})_2Co$ completely decomposes over the course of several minutes. In contrast, solid samples of $(Cp^{4i})_2Co$ are indefinitely stable in air (>6 months). Solutions of $(Cp^{4i})_2Co$ exposed to oxygen slowly decompose over the course of several minutes, however. The higher air stability of $(Cp^{4i})_2Co$ is undoubtedly due to the encapsulation of the metal center by the extremely bulky $[Cp^{4i}]^-$ ligands. Similar air stability has been reported for octaphenylcobaltocene $(Ph_4C_5H)_2Co$,[18] which is also indefinitely air stable as a solid and is only partly decomposed after 12 h of exposure to oxygen in solution.

Synthesis of $[(Cp^{3i})_2Fe]BF_4$ and $[(Cp^{4i})_2Fe]BF_4$. Oxidation of $(Cp^{3i})_2Fe$ and $(Cp^{4i})_2Fe$ with excess $NOBF_4$ in methylene chloride gave the corresponding ferrocenium tetrafluoroborate complexes, $[(Cp^{3i})_2Fe]BF_4$ and

(15) Ironically, a dramatic improvement (yields >85%) in the synthesis of Cp^*_2Co could be effected by conducting the reaction of $LiCp^*$ with $CoBr_2$(dme) in a *refluxing* mixture of THF and Et_2O. See ref 16.

(16) Koelle, U.; Khouzami, F. *Angew. Chem., Int. Ed. Engl.* **1980**, *19*, 640−641.

(17) Robbins, J. L.; Edelstein, N.; Spencer, B.; Smart, J. C. *J. Am. Chem. Soc.* **1982**, *104*, 1882−1893.

(18) Castellani, M. P.; Geib, S. J.; Rheingold, A. L.; Trogler, W. C. *Organometallics* **1987**, *6*, 1703−1712.

$[(Cp^{4i})_2Fe]BF_4$, in excellent yield (eq 2).[19] The formation

$$(Cp^{ni})_2Fe + NOBF_4 \xrightarrow{CH_2Cl_2} [(Cp^{ni})_2Fe]BF_4 + NO(g)\uparrow \quad (2)$$

of $[(Cp^{3i})_2Fe]BF_4$ was rapid, occurring essentially on mixing, whereas for $(Cp^{4i})_2Fe$, several hours were required before the oxidation was complete. Recrystallization of the crude products from CH_2Cl_2/Et_2O mixtures at −20 °C gave both $[(Cp^{3i})_2Fe]BF_4$ and $[(Cp^{4i})_2Fe]BF_4$ as air-stable, forest-green solids.

Magnetic susceptibility measurements at room temperature in THF-d_8 confirmed the paramagnetic nature of the complexes; the values for $[(Cp^{3i})_2Fe]BF_4$ and $[(Cp^{4i})_2Fe]BF_4$ were 2.68 and 2.27 μ_B, respectively. These values are higher than the spin-only value of 1.73 μ_B expected for complexes with one unpaired electron, but are typical of the values found for ferrocenium complexes (cf. 2.44 μ_B for $[Cp_2Fe]BF_4$ and 2.59 μ_B for $[Cp_2Fe]PF_6$[20]), and reflect a substantial angular orbital contribution to the magnetic moment.[21]

Synthesis of $[(Cp^{3i})_2Co]X$ and $[(Cp^{4i})_2Co]X$ (X = PF_6 and BPh_4). Oxidation of the neutral cobaltocenes $(Cp^{3i})_2Co$ and $(Cp^{4i})_2Co$ with an excess of either NH_4PF_6 or NH_4BPh_4 in THF gave the corresponding cobaltocenium complexes $[(Cp^{3i})_2Co]X$ and $[(Cp^{4i})_2Co]X$ (X = PF_6, BPh_4) in high yield (eq 3).

$$(Cp^{ni})_2Co + [NH_4]X \xrightarrow[n = 3,4\ X = PF_6,\ BPh_4]{THF} [(Cp^{ni})_2Co]X + NH_3 + {}^1/_2\ H_2(g)\uparrow \quad (3)$$

As was the case for their iron counterparts, the oxidation reaction was noticeably slower for $(Cp^{4i})_2Co$, typically requiring 18−24 h to ensure completion, compared to the 4 h needed for $(Cp^{3i})_2Co$. Separation of the crude products from the excess ammonium salts, either by washing with water ($[PF_6]^-$) or chloroform extraction ($[BPh_4]^-$), followed by recrystallization from acetone/Et_2O yielded the cobaltocenium complexes as yellow to orange, air-stable solids.

The cobaltocenium complexes were characterized by NMR (^1H and ^{13}C) and IR spectroscopies. Proton and ^{13}C NMR spectra were similar to those seen for other diamagnetic $(Cp^{3i})_2M$ and $(Cp^{4i})_2M$ metallocenes.[2,3] Broadening of the resonances was seen in the room temperature NMR spectra of the $[(Cp^{4i})_2Co]X$ complexes; a well-resolved proton NMR spectrum (DMSO-d_6) for $[(Cp^{4i})_2Co]BPh_4$ could be obtained at 60 °C. The broadening at room temperature is most likely due to hindered rotation of the $[Cp^{4i}]^-$ rings and/or the isopropyl substituents on them,[22,23] and attests to the severity of the steric congestion brought about by the bulky $[Cp^{4i}]^-$ ligands.[24]

Table 8. Electrochemical Data for $(Cp^{3i})_2M$ and $(Cp^{4i})_2M$ (M = Fe, Co)

redox couple	$E_{1/2}$ (V)	$\lvert E_{ox} - E_{red}\rvert$ (mV)	ref
$Cp_2Fe/[Cp_2Fe]^+$	+0.44	72[a]	27
$(Cp^{3i})_2Fe/[(Cp^{3i})_2Fe]^+$	+0.25	158[b]	this work
$(Cp^{4i})_2Fe/[(Cp^{4i})_2Fe]^+$	+0.06	122[b]	this work
$Cp^*_2Fe/[Cp^*_2Fe]^+$	−0.12	82[a]	27
$Cp_2Co/[Cp_2Co]^+$	−0.86	*c*	16
$(Cp^{3i})_2Co/[(Cp^{3i})_2Co]^+$	−1.15	165[a]	this work
$(Cp^{4i})_2Co/[(Cp^{4i})_2Co]^+$	−1.14	163[a]	this work
$Cp^*_2Co/[Cp^*_2Co]^+$	−1.48	*c*	16

[a] At 0.1 V s^{-1}. [b] At 0.2 V s^{-1}. [c] Not given.

Electrochemistry of Iron and Cobalt Metallocenes. The effect of the $[Cp^{3i}]^-$ and $[Cp^{4i}]^-$ ligands on the electrochemical properties of the corresponding iron and cobalt metallocenes was studied using cyclic voltammetry. Voltammograms were obtained for 2 mM CH_2Cl_2 solutions of $(Cp^{3i})_2Fe$, $(Cp^{4i})_2Fe$, $[(Cp^{3i})_2Co]^+$, and $[(Cp^{4i})_2Co]^+$; the potentials for the $(Cp^{4i})_2M^{0/+1}$ redox couples, along with the analogous potentials for the Cp_2M and Cp^*_2M metallocenes, are listed in Table 8.

$(Cp^{3i})_2Fe$ undergoes a quasi-reversible oxidation[25−27] at +0.25 V (vs SCE) in CH_2Cl_2; for $(Cp^{4i})_2Fe$, this oxidation has shifted cathodically to +0.06 V. In contrast, the analogous cobaltocenes undergo quasi-reversible oxidations at virtually identical potentials: −1.15 V (vs SCE) for $(Cp^{3i})_2Co$ and −1.14 V for $(Cp^{4i})_2Co$, in spite of the different cyclopentadienyl ligands. As expected, given the partial alkyl substitution of the $[Cp^{3i}]^-$ and $[Cp^{4i}]^-$ ligands, the oxidation potentials for all $(Cp^{3i})_2M$ and $(Cp^{4i})_2M$ metallocenes are between those of the corresponding unsubstituted Cp_2M and fully alkylated Cp^*_2M complexes (Table 8).

Solid State Structures. $(Cp^{3i})_2Fe$. During the course of this work, X-ray quality crystals of the previously reported ferrocene complex $(Cp^{3i})_2Fe$ [5] were obtained. The molecule displays a rigorously planar sandwich geometry, with a crystallographically imposed center of inversion at the iron atom (Figure 1).

The structural parameters of $(Cp^{3i})_2Fe$ indicate that the six isopropyl substituents are able to arrange themselves to avoid any significant steric crowding in the complex. The average Fe-C bond distance in $(Cp^{3i})_2Fe$ of 2.05(1) Å is the same as that in ferrocene (2.05 Å)[28,29] and Cp^*_2Fe (2.050(2) Å).[30] Additionally, the closest inter-ring contact involving the isopropyl groups is 3.93 Å (between C(7) and C(10′), which is only slightly less than the sum of the van der Waals radii for two methyl groups (40 Å).[27] The one concession made by the complex to accommodate the two $[Cp^{3i}]^-$ ligands is that the isopropyl methane carbons are bent out of the ring plane more than would be expected in the absence of any crowding; their 0.12 Å average

(19) Zanello, P.; Cinquantini, A.; Mangani, S.; Opomolla, G.; Pardi, L.; Janiak, C.; Rausch, M. D. *J. Organomet. Chem.* **1994**, *471*, 171−177.
(20) Sohn, Y. S.; Hendrickson, D. N.; Gray, H. B. *J. Am. Chem. Soc.* **1970**, *92*, 3233−3234.
(21) Cotton, F. A.; Wilkinson, G. *Advanced Inorganic Chemistry*, 5th ed.; Wiley: New York, 1988.
(22) Gloaguen, B.; Astruc, D. *J. Am. Chem. Soc.* **1990**, *112*, 4607−4609.
(23) Buchholz, D.; Astruc, D. *Angew. Chem., Int. Ed. Engl.* **1994**, *33*, 1637−1639.
(24) Sitzmann has placed the barrier to ring rotation in $(Cp^{4i})_2Fe$ at 13.6 kcal/mol. See ref 5.
(25) On the basis of the behavior of other ferrocene and cobaltocene derivatives (refs 26 and 27), these are presumably one-electron oxidations. The quasi-reversibility (as suggested by the peak-to-peak separations) may be partially a consequence of uncompensated solvent resistance; see ref 27.
(26) El Murr, N. *J. Organomet. Chem.* **1976**, *112*, 189−199.
(27) Gallucci, J. C.; Opromolla, G.; Paquette, L. A.; Pardi, L.; Schirch, P. F. T.; Sivik, M. R.; Zanello, P. *Inorg. Chem.* **1993**, *32*, 2292−2297.
(28) Seiler, P.; Dunitz, J. D. *Acta. Crystallogr., Sect. B* **1979**, *B35*, 1068−1074.
(29) Takusagawa, F.; Koetzle, T. F. *Acta Crystallogr., Sect. B* **1979**, *B35*, 1074−1081.
(30) Freyberg, D. P.; Robbins, J. L.; Raymond, K. N.; Smart, J. C. *J. Am. Chem. Soc.* **1979**, *101*, 892−897.

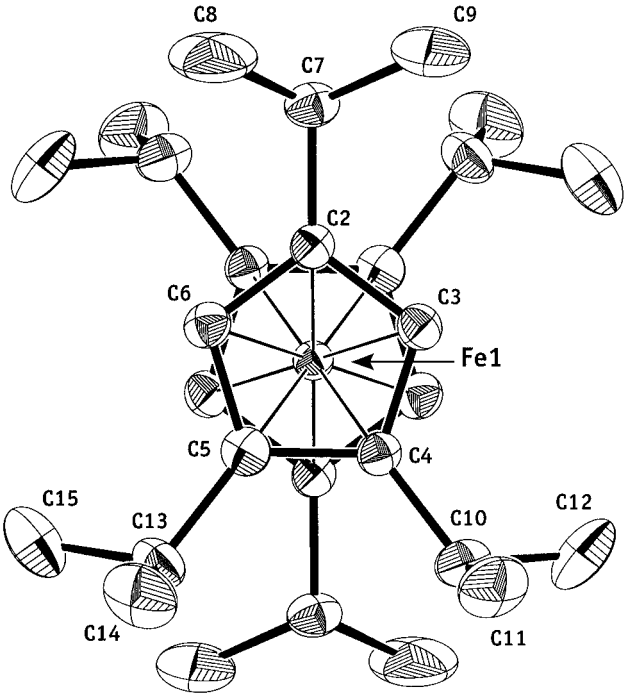

Figure 1. ORTEP diagram of the non-hydrogen atoms of $(Cp^{3i})_2Fe$, giving the numbering scheme used in the text. Thermal ellipsoids are shown at the 30% level.

displacement is almost double the analogous 0.064 Å displacement observed for the methyl groups in Cp^*_2Fe.[26]

The three unique isopropyl substituents in $(Cp^{3i})_2Fe$ exhibit orientation angles[31] of 70.0°, 63.5°, and 21.7° with respect to the cyclopentadienyl ring plane. The latter, nearly coplanar angle is for the C(7)−C(8)−C(9) isopropyl group, which has both methyl carbons above the ring plane away from the Fe atom (Figure 1). The ability of the $[Cp^{3i}]^-$ ligands to assume a conformation with such an arrangement of the isopropyl groups greatly reduces steric congestion at the metal center.

$(Cp^{3i})_2Co$. Crystals of $(Cp^{3i})_2Co$ are isomorphous with those of $(Cp^{3i})_2Fe$, and the two molecules are isostructural (Figure 2). As is the case for $(Cp^{3i})_2Fe$, the average Co-C(ring) distance of 2.122(7) Å is indistinguishable from the average metal−carbon distances in both Cp_2Co (2.096(8) Å)[32] and Cp^*_2Co (2.105(2) Å)[33] at the 3σ level. However, there is less bending of the isopropyl methine carbons out of the ring plane in $(Cp^{3i})_2Co$ (average of 0.08 Å) than was found for $(Cp^{3i})_2Fe$, which is most likely a consequence of the slightly longer M-C(ring) bonds in $(Cp^{3i})_2Co$.

$[(Cp^{3i})_2Fe]BF_4$. An X-ray structural determination of $[(Cp^{3i})_2Fe]BF_4$ revealed two $[(Cp^{3i})_2Fe]^+$ cations at half-occupancy and one $[BF_4]^-$ ion at full-occupancy per asymmetric unit. Each $[(Cp^{3i})_2Fe]^+$ cation contained a crystallographically imposed inversion center. An ORTEP view of the relative orientations of the $[(Cp^{3i})_2Fe]^+$ cations and $[BF_4]^-$ anion is given in Figure 3.

The $[(Cp^{3i})_2Fe(1)]^+$ cation displays an average Fe-C(ring) distance of 2.08(2) Å, which is equivalent to the average Fe-C(ring) distance of 2.09 Å for several deca-

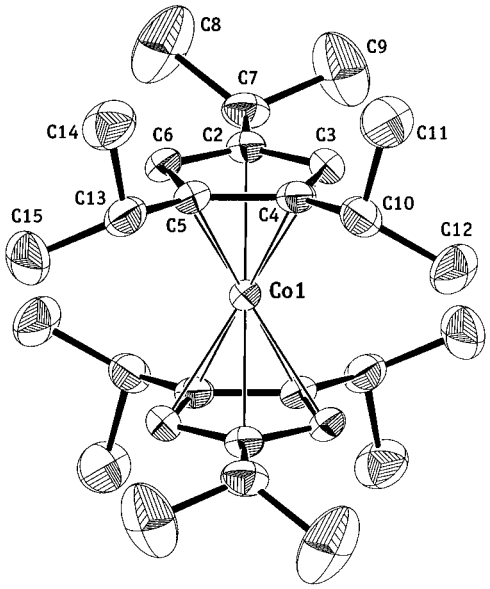

Figure 2. ORTEP diagram of the non-hydrogen atoms of $(Cp^{3i})_2Co$, giving the numbering scheme used in the text. Thermal ellipsoids are displayed at the 30% level.

methylferrocenium complexes, $[Cp^*_2Fe]X$.[34−37] The variation in the individual Fe(1)-C(ring) distances is small ($\Delta_{M\text{-}C}$ = 0.03 Å), and the *ipso* carbons of the isopropyl groups are displaced by an average of 0.13 Å away from the ring plane, essentially the same as in the neutral $(Cp^{3i})_2Fe$ (0.12 Å). Although the average Fe(2)-C(ring) distance in the second cation (2.10(2) Å) is indistinguishable from that in the first, there is more variation in the values, from 2.04(1) to 2.13(1) Å ($\Delta_{M\text{-}C}$ = 0.09 Å). The *ipso* carbons of the isopropyl groups are displaced by an average of 0.10 Å. The variations between the two ferrocenium cations can only be a consequence of crystal packing, so the differences observed in the variation of Fe-C lengths provide a useful benchmark for establishing the chemical significance of ring slippage.

$[(Cp^{3i})_2Co]BPh_4$. An X-ray structural determination of $[(Cp^{3i})_2Co]BPh_4$ revealed that both the cation and the anion possess crystallographically imposed symmetry; i.e., a 2-fold rotation axis through the cobalt atom for $[(Cp^{3i})_2Co]^+$ and a $\bar{4}$ rotation axis through the boron atom for $[BPh_4]^-$. An ORTEP view of the cation of $[(Cp^{3i})_2Co]BPh_4$ is shown in Figure 4.

The orientation of the $[Cp^{3i}]^-$ ligands in $[(Cp^{3i})_2Co]BPh_4$ is different from the planar, staggered $[Cp^{3i}]^-$ rings found in $(Cp^{3i})_2Fe$ and $(Cp^{3i})_2Co$; the rings are more nearly eclipsed (twist angle of 18.4°) and are slightly nonparallel (ring centroid-Co-ring centroid angle of 177.9° and ring normal-Co-ring normal angle of 174.7°). The more eclipsed arrangement of the rings in $[(Cp^{3i})_2Co]BPh_4$ brings the isopropyl groups on the C(2) and C(4)′ ring carbons into relatively close contact, as the separation between the two methine carbons of

(31) The orientation of an *i*-Pr group is found by calculating the angle between the ring plane and the plane formed by the two methyl carbons of an *i*-Pr group and its adjacent ring carbon.

(32) Bünder, W.; Weiss, E. *J. Organomet. Chem.* **1975**, *92*, 65−68.
(33) Haaland, A. *Acc. Chem. Res.* **1979**, *12*, 415−422.
(34) Dixon, D. A.; Calabrese, J. C.; Miller, J. S. *J. Am. Chem. Soc.* **1986**, *108*, 2582−2588.
(35) Gebert, E.; Reis, A. H., Jr.; Miller, J. S.; Rommelmann, H.; Epstein, A. J. *J. Am. Chem. Soc.* **1982**, *104*, 4403−4410.
(36) Miller, J. S.; Zhang, J. H.; Reiff, W. M.; Dixon, D. A.; Preston, L. D.; Reis, A. H., Jr.; Gebert, E.; Extine, M.; Troup, J.; Epstein, A. J.; Ward, M. D. *J. Phys. Chem.* **1987**, *91*, 4344−4360.
(37) Miller, J. S.; Calabrese, J. C.; Harlow, R. L.; Dixon, D. A.; Zhang, J. H.; Reiff, W. M.; Chittipeddi, S.; Selover, M. A.; Epstein, A. J. *J. Am. Chem. Soc.* **1990**, *112*, 5496−5506.

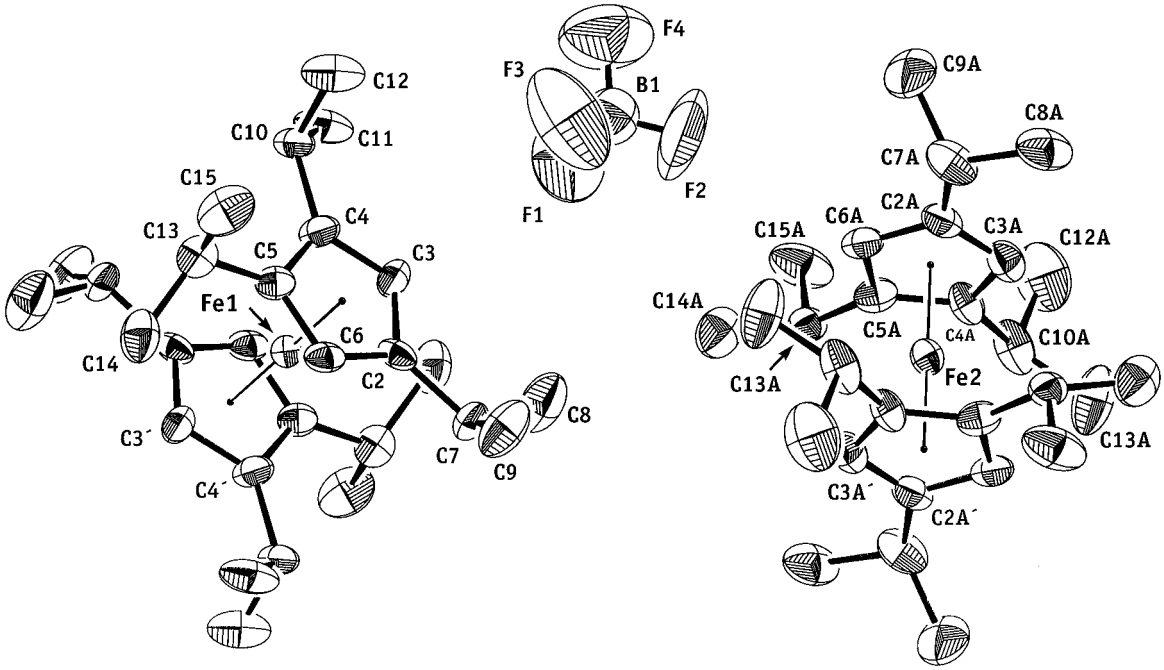

Figure 3. ORTEP diagram of the non-hydrogen atoms of the two independent molecules of $[(Cp^{3i})_2Fe]BF_4$, giving the numbering scheme used in the text. Thermal ellipsoids are shown at the 30% level.

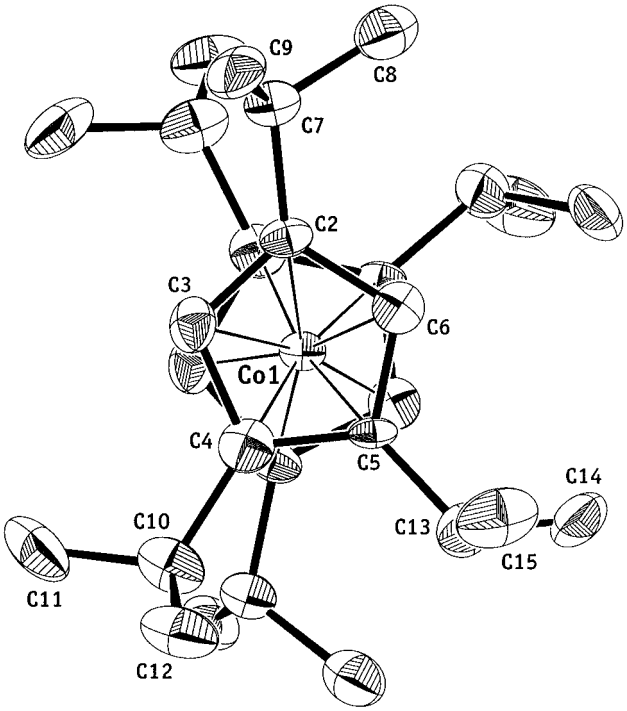

Figure 4. ORTEP diagram of the non-hydrogen atoms of the $[(Cp^{3i})_2Co]^+$ cation ($[BPh_4]^-$ salt), giving the numbering scheme used in the text. Thermal ellipsoids are displayed at the 35% level.

these groups (C(7) and C(10)′) is only 3.59 Å. However, all other inter-ring contacts between the isopropyl groups are longer than 3.9 Å.

The average Co-C distance of 2.05(1) Å in $[(Cp^{3i})_2Co]BPh_4$ is identical to that observed in several $[Cp^*_2Co]X$ complexes[37,38] and is also the same as the average Fe-C(ring) distance in $(Cp^{3i})_2Fe$. Interestingly, the average Co-C(ring) distance in $[(Cp^{3i})_2Co]BPh_4$ is somewhat longer than the analogous distance of 2.013(7) Å observed for the unsubstituted cobaltocenium cation in $[Cp_2Co][CpMo(NO)_2Et]$.[39]

$[(Cp^{4i})_2Fe]BF_4$. To date, we have not been able to grow crystals of $(Cp^{4i})_2Fe$ suitable for characterization by X-ray diffraction. However, X-ray quality crystals of the corresponding ferrocenium cation, $[(Cp^{4i})_2Fe]BF_4$, could be obtained. An X-ray structural determination of the complex revealed one $[(Cp^{4i})_2Fe]^+$ and $[BF_4]^-$ ion per asymmetric unit. An ORTEP view of the $[(Cp^{4i})_2Fe]^+$ cation is given in Figure 5.

In contrast to $[(Cp^{3i})_2Fe]BF_4$, the structure of $[(Cp^{4i})_2Fe]BF_4$ exhibits several features indicative of substantial inter-ring repulsions between the $[Cp^{4i}]^-$ ligands. The average Fe-C distance of 2.14(1) Å is somewhat longer than the corresponding distances in $[(Cp^{3i})_2Fe]^+$ (2.08(2) and 2.10(2) Å) and in several unsubstituted ferrocenium salts, $[Cp_2Fe]X$ (2.05−2.08 Å),[40] although the estimated standard deviations make the difference of limited crystallographic significance. Only in the complexes $[(Ph_5C_5)_2Fe]BF_4$[41] and $\{[(Me_3Si)_3C_5H_2]Fe\}BF_4$[42] is a similar lengthening of the Fe-Cp′ interaction observed; the steric repulsion of the bulky substituents on the rings leads to average Fe-C(ring) distances of 2.16(1) and 2.137 Å, respectively. The Fe-C(ring) bond lengths for the unsubstituted carbon atoms (both 2.10(1) Å) in $[(Cp^{4i})_2Fe]BF_4$ are shorter than those of the isopropyl-substituted carbon atoms, which range from 2.13(1) to 2.18(1) Å. An analogous pattern of Fe-C(ring) bond distances is found for octaphenylferrocene $(Ph_4C_5H)_2Fe$; i.e., 2.054(3) Å for Fe-C(H) and 2.088(3)−2.099(3) Å for Fe-C(Ph).[43]

(38) Dixon, D. A.; Miller, J. S. *J. Am. Chem. Soc.* **1987**, *109*, 3656−3664.

(39) Legzdins, P.; Wassink, B.; Einstein, F. W. B.; Jones, R. H. *Organometallics* **1988**, *7*, 477−481.

(40) Martinez, R.; Tiripicchio, A. *Acta Crystallogr., Sect. C* **1990**, *46*, 202−205 and references therein.

(41) Schumann, H.; Lentz, A.; Weimann, R.; Pickardt, J. *Angew. Chem., Int. Ed. Engl.* **1994**, *33*, 1731−1733.

(42) Okuda, J.; Albach, R. W.; Herdtweck, E.; Wagner, F. E. *Polyhedron* **1991**, *10*, 1741−1748.

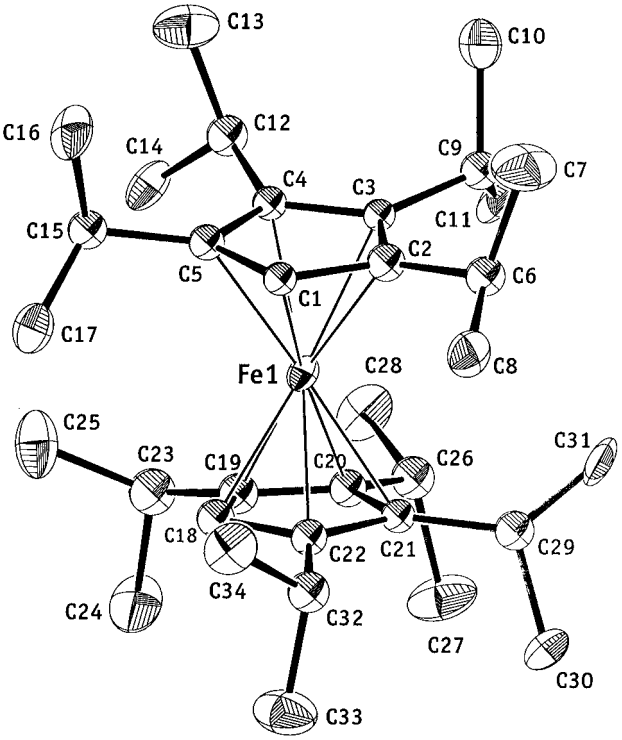

Figure 5. ORTEP diagram of the non-hydrogen atoms of $[(Cp^{4i})_2Fe]BF_4$, giving the numbering scheme used in the text. Thermal ellipsoids are shown at the 35% level; the $[BF_4]^-$ anion has been omitted for clarity.

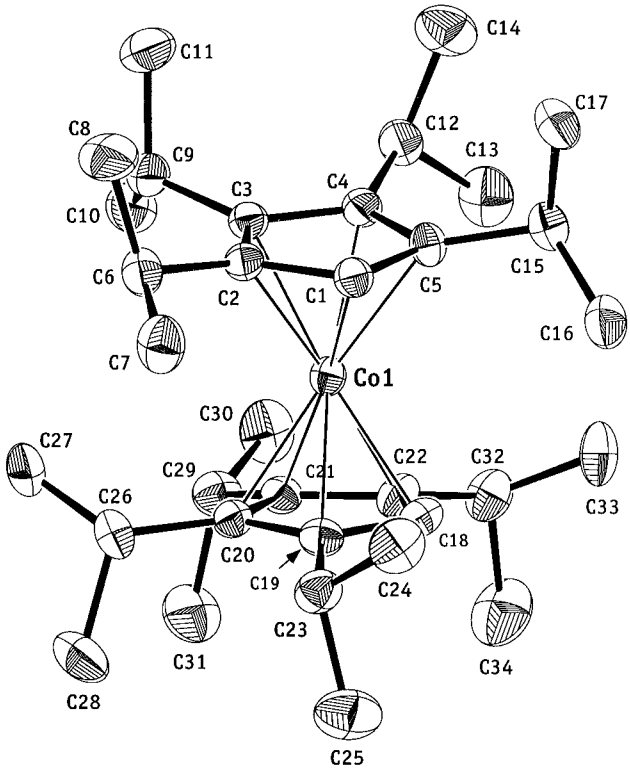

Figure 6. ORTEP diagram of the non-hydrogen atoms of the $[(Cp^{4i})_2Co]^+$ cation ($[PF_6]^-$ salt), giving the numbering scheme used in the text. Thermal ellipsoids are displayed at the 35% level.

The steric congestion present in $[(Cp^{4i})_2Fe]BF_4$ also causes the isopropyl substituents to be bent substantially out of the ring plane away from the iron atom. The average displacement of the methine isopropyl carbons out of the ring plane is 0.23 Å, double the 0.10−0.13 Å average displacement seen in $[(Cp^{3i})_2Fe]BF_4$ and equivalent to a bending angle (α) of 8.7°. An identical average displacement of 0.23 Å is found for the *ipso* carbons of the phenyl substituents in $[(Ph_5C_5)_2Fe]BF_4$; apparently, the steric strain caused by the Cp ligands in both $[(Ph_5C_5)_2Fe]BF_4$ and $[(Cp^{4i})_2Fe]BF_4$ is roughly the same. In spite of the lengthening of the Fe-C distances and the bending of the isopropyl groups away from the iron atom in $[(Cp^{4i})_2Fe]BF_4$, there are still several close (<3.6 Å) inter-ring contacts involving the isopropyl groups.

The $[Cp^{4i}]^-$ rings in $[(Cp^{4i})_2Fe]BF_4$ are distinctly nonparallel, with ring centroid-Fe-ring centroid and ring normal-Fe-ring normal angles of 174.3° and 170.7°, respectively. As in the main-group metallocenes $(Cp^{4i})_2Ca$ [1] and $(Cp^{4i})_2Sn$,[2] the $[Cp^{4i}]^-$ ligands are bent toward the two unsubstituted carbons (C(1) and C(18)) of the ring. The almost 10° tilt of the rings in $[(Cp^{4i})_2Fe]BF_4$ makes it the most distorted ferrocenium complex yet reported; it stands in contrast to the linear (or nearly linear) arrangements normally observed for ferrocene and ferrocenium compounds. Even $[(Ph_5C_5)_2Fe]BF_4$ and $(Ph_4C_5H)_2Fe$, with cyclopentadienyl ligands bulky enough to lengthen the Fe-C bond distances, have planar geometries. Excluding *ansa*-bridged metallocenes, the only other reported iron metallocene complexes with significantly bent Cp ligands are $[(Me_3Si)_3C_5H_2]_2Fe$ [44] and the TCNQ salt of bis(η^5-tricyclo[5.2.1.$0^{2,6}$]deca-2,5,8-trien-6-yl)iron,[27] which have ring normal-Fe-ring normal angles of 173.9° and 172.9°, respectively. Like $[(Cp^{4i})_2Fe]BF_4$, the bent angles in these complexes have been ascribed to inter-ring steric repulsions between the cyclopentadienyl substituents.

$[(Cp^{4i})_2Co]PF_6$. The orientation of the $[Cp^{4i}]^-$ rings in $[(Cp^{4i})_2Co]PF_6$ (Figure 6) is nearly identical to that found for the $[(Cp^{4i})_2Fe]^+$ cation, with ring centroid-Co-ring centroid and ring normal-Co-ring normal angles of 174.8° and 171.5°, respectively, and a 0.25 Å average displacement of the methine isopropyl carbons from the ring plane. Apparently, this particular arrangement best helps to relieve the severe inter-ring repulsions between the $[Cp^{4i}]^-$ ligands in these complexes.

The average Co-C distance in $[(Cp^{4i})_2Co]PF_6$ is 2.09(1) Å, the longest such value yet observed for a cobaltocenium complex. This value is nearly identical to the average Co-C distance for neutral cobaltocene, Cp_2Co (2.096(8) Å).[32] The only other reported cobalt-based metallocene that exhibits a significant lengthening of the Co-C bonds owing to steric crowding is octaphenylcobaltocene, which has an average Co-C distance of 2.15(1) Å.[18]

Discussion

Comparison of $(Cp^{3i})_2M$ and $(Cp^{4i})_2M$. Main-group metallocenes containing tri- and tetraisopropyl-(cyclopentadienyl) rings display marked differences in their physical properties.[2,4] This distinction is not retained in the corresponding iron and cobalt complexes, however, as the physical characteristics of the $(Cp^{3i})_2M$ (M = Fe, Co) metallocenes are essentially the same as those of $(Cp^{4i})_2M$ (e.g., all complexes are relatively high

(43) Castellani, M. P.; Wright, J. M.; Geib, S. J.; Rheingold, A. L.; Trogler, W. C. *Organometallics* **1986**, *5*, 1116−1122.
(44) Okuda, J.; Herdtweck, E. *Chem. Ber.* **1988**, *121*, 1899−1905.

melting (>135 °C), readily crystallized solids).[5] This result most likely reflects the increased amount of intramolecular contact between the two $[Cp^{3i}]^-$ ligands in $(Cp^{3i})_2M$, a consequence of the shorter M-C(ring) bonds to the smaller transition metals. The greater contact decreases the conformational flexibility of the $[Cp^{3i}]^-$ ligands, improving lattice packing and leading to the higher melting points and greater crystallinity of the metallocenes.[4,45]

In addition to their differences in physical characteristics, main-group $(Cp^{3i})_2M'$ and $(Cp^{4i})_2M'$ complexes (M′ = Mg, Ca, Sr, Ba, Sn, Pb) also display conspicuous variations in reactivity.[4,45,46] In this respect, the transition metal complexes are similar. The contrasting air stability of solid $(Cp^{4i})_2Co$ (indefinite) and $(Cp^{3i})_2Co$ (minutes) constitutes one obvious example; other differences are found in the fact that the oxidation of the metal center by NO^+ (or NH_4^+) is slower for $(Cp^{4i})_2Fe$ ($(Cp^{4i})_2Co$) than for $(Cp^{3i})_2Fe$ ($(Cp^{3i})_2Co$). Thus, the two $[Cp^{4i}]^-$ ligands effectively "encapsulate" the metal center in the $(Cp^{4i})_2M$ complexes, retarding the reactivity of these complexes with even small reagents such as O_2. The removal of an isopropyl group from each ring on going to $(Cp^{3i})_2M$, however, results in complete loss of metal encapsulation; the reactivity of these complexes is similar to that observed for iron and cobalt metallocenes with unhindered Cp ligands.[47]

As with their main group analogues, the distinctive reactivity of $(Cp^{4i})_2M$ and $(Cp^{3i})_2M$ (M = Fe, Co) can be traced to intrinsic characteristics of the $[Cp^{3i}]^-$ and $[Cp^{4i}]^-$ ligands. Specifically, the isopropyl groups in the $[Cp^{4i}]^-$ ligand are limited to a nearly perpendicular orientation relative to the C_5 ring plane; this maximizes the steric bulk of the ligand at the metal center and leads to its almost complete encapsulation. In contrast, the isopropyl substituents in the $[Cp^{3i}]^-$ ligand are not as constrained to perpendicular arrangements. This is most apparent in the solid state structures of $(Cp^{3i})_2Fe$ and $(Cp^{3i})_2Co$, where two of the isopropyl groups lie nearly in the plane of the cyclopentadienyl rings, with the methyl groups pointed away from the metal (Figures 1 and 2). This substantially reduces the steric congestion at the metal center in $(Cp^{3i})_2M$, and thus, the effects of metal encapsulation on reactivity are lost.

It is noteworthy that the differences in reactivity observed for the main-group $(Cp^{3i})_2M'$ and $(Cp^{4i})_2M'$ metallocenes are retained in the analogous iron and cobalt complexes, despite the smaller size of the transition metals. This indicates that the increased amount of inter-ring contact between the two $[Cp^{3i}]^-$ ligands in $(Cp^{3i})_2M$ is not enough to enforce an encapsulating arrangement; apparently, at least four isopropyl groups per ring are needed to generate encapsulated complexes with chemically distinctive properties.

Steric Strain in $[(Cp^{4i})_2M]^+$. Although the $[Cp^{4i}]^-$ ligand is bulky enough to influence the reactivity of main-group $(Cp^{4i})_2M'$ metallocenes, it does not cause any significant steric strain in these complexes; the metal−carbon bond lengths in $(Cp^{4i})_2M'$ are similar to those found for other metallocenes of these metals.[48] However, for the smaller transition metals, there are now several indications of severe steric crowding in the $(Cp^{4i})_2M$ metallocenes. One indication of crowding is the substantial bending of the isopropyl substituents away from the C_5 ring plane in the solid state structures of $[(Cp^{4i})_2M]^+$ (M = Fe, Co). Distortions in the metal−Cp bonding are also observed; unlike most transition metal metallocenes, the two $[Cp^{4i}]^-$ ligands in $[(Cp^{4i})_2M]^+$ are significantly bent (ca. 10°), in both cases toward the unsubstituted ring carbons. Additionally, the $[Cp^{4i}]^-$ ligands are tipped away from the metal; although the M-C(H) bond lengths in $[(Cp^{4i})_2M]^+$ are similar to those in $[(Cp^{3i})_2M]^+$ and $[Cp^*_2M]^+$, the M-C(*i*Pr) bond lengths are noticeably longer. This leads to an overall lengthening (ca. 0.05 Å) of the average M-C(ring) bond distances in $[(Cp^{4i})_2M]^+$ relative to those in $[(Cp^{3i})_2M]^+$ and $[Cp^*_2M]^+$.

The elongation of the covalent metal−Cp bonds in $[(Cp^{4i})_2M]^+$ attests to the severity of the steric crowding present at the metal center in these complexes.[49] Previously, only $[Ph_4C_5H]^-$,[18,43] $[Ph_5C_5]^-$,[41] and $[(Me_3Si)_3C_5H_2]^-$ [42] were known to be bulky enough to cause an appreciable lengthening of the metal−Cp bond in transition metal metallocenes. The ca. 171° interplanar angles of the $[(Cp^{4i})_2Fe]^+$ and $[(Cp^{4i})_2Co]^+$ complexes also place them among the most bent of any transition metal Cp'_2M complexes; bending is not observed in the $(Ph_4C_5H)_2M$ and $(Ph_5C_5)_2M$ complexes.

The steric overcrowding in the $(Cp^{4i})_2M$ and $[(Cp^{4i})_2M]^+$ complexes appears to cause more than structural distortions; it also seems to influence the electrochemical potentials of these compounds. This is most obvious for the cobalt metallocenes, in that $[(Cp^{4i})_2Co]^+$ has essentially the same oxidation potential as $[(Cp^{3i})_2Co]^+$ ($\Delta E° < 0.01$ V), despite the two additional electron-donating isopropyl groups in the $[(Cp^{4i})_2Co]^+$ complex.[50] For the iron complexes, this is not as obvious, as $(Cp^{4i})_2Fe$ is more readily oxidized than $(Cp^{3i})_2Fe$, in line with the expected electronic effects of the ligands. However, considering the 190 mV difference in the oxidation potential between Cp_2Fe (0.44 V) and $(Cp^{3i})_2Fe$ (0.25 V), the fact that the same difference is seen for $(Cp^{3i})_2Fe$ and $(Cp^{4i})_2Fe$ (0.06 V) suggests that the oxidation of $(Cp^{4i})_2Fe$ is more energetically favorable than would normally be accounted for by the two additional isopropyl groups.[50−52]

The most plausible reason for the anomalous potentials for $[(Cp^{4i})_2M]^{0/+}$ is the steric crowding that is present in these complexes. For both iron and cobalt, it is the generation of the complex in the redox couple with *the longer M-C(ring) bonds* (e.g., the 19-electron $(Cp^{4i})_2Co$ and the 17-electron $[(Cp^{4i})_2Fe]^+$) that has become energetically more favorable than would be

(45) Burkey, D. J.; Hanusa, T. P. *Comments Inorg. Chem.* **1995**, *17*, 41−77.
(46) Burkey, D. J.; Hanusa, T. P.; Huffman, J. C. Unpublished results.
(47) Pearson, A. J. *Metallo-organic Chemistry*; Wiley: New York, 1985.
(48) An exception to this statement is provided by the slipped structure of $[(C_3H_7)_4C_5H]_2Zn$, which appears to be a consequence of steric interaction between the rings; see ref 49.
(49) Burkey, D. J.; Hanusa, T. P. *J. Organomet. Chem.* **1996**, *512*, 165−173.
(50) Slocum, D. W.; Ernst, C. R. *Adv. Organomet. Chem.* **1972**, *10*, 79−114.
(51) It should be noted that the 0.19 V potential difference between $(Cp^{3i})_2Fe$ and $(Cp^{4i})_2Fe$ is almost twice as large as the 0.1 V difference reported for Cp_2Fe and $[(i\text{-Pr})C_5H_4]_2Fe$ (ref 52), further supporting the contention that the steric strain present in $(Cp^{4i})_2Fe$ renders oxidation of this complex more favorable.
(52) Little, W. F.; Reilley, C. N.; Johnson, J. D.; Sanders, A. P. *J. Am. Chem. Soc.* **1964**, *86*, 1382−1386.

expected based solely on electronic effects. Thus, the partial relief of steric strain on going from $[(Cp^{4i})_2Co]^+$ to $(Cp^{4i})_2Co$ or from $(Cp^{4i})_2Fe$ to $[(Cp^{4i})_2Fe]^+$ provides an energetic benefit that is reflected in the corresponding electrochemical potentials.

Although the electronic effects of the ring substituents on the electrochemical potentials of metallocene complexes has long been recognized,[19,50] the influence of steric crowding on the potentials has not been as well documented.[27,42] One example that correlates with our results on $(Cp^{4i})_2M$ is the oxidation potential of octaphenylferrocene,[43] which is only 0.03 V more positive than that for ferrocene in spite of the presence of the electron-withdrawing $[Ph_4C_5H]^-$ ligands. Considering that 1,1′,3,3′-tetraphenylferrocene, with only four phenyl substituents, has an oxidation potential that is 0.11 V more positive than that for ferrocene,[53] it appears that steric crowding renders the oxidation of $[Ph_4C_5H]_2Fe$ (with its subsequent lengthening of the Fe-C(ring) bonds) more favorable than would be expected given the electronic nature of the ring substituents. Similarly, the oxidation potentials of $((Me_3Si)_3C_5H_2)FeCp$ and $[(Me_3Si)_3C_5H_2]_2Fe$ are shifted by 0.017 and −0.104 V relative to ferrocene, respectively;[42] the cathodic shift of the potential for $[(Me_3Si)_3C_5H_2]_2Fe$ was ascribed to the relief of steric congestion that occurs on oxidation.

Conclusions

The characteristics of the $(Cp^{3i})_2M$ and $(Cp^{4i})_2M$ metallocenes have demonstrated the conspicuous effects that the difference of a single isopropyl group can have on transition metal complexes that contain the $[Cp^{3i}]^-$ and $[Cp^{4i}]^-$ ligands. The increased encapsulation of the metal center in the $(Cp^{4i})_2M$ complexes enhances their air stability, but the greater steric repulsions between the rings induces marked structural distortions not present in the $[(Cp^{3i})_2M]^{0/+}$ compounds. The steric congestion in the $(Cp^{4i})_2M$ complexes also influences the electrochemical potentials of these compounds, providing an energetic benefit for the oxidation state with longer metal−carbon bond lengths. These results suggests that steric control of the reactivity may become an important feature of the chemistry of encapsulated transition metal metallocenes. Further investigations into the intriguing characteristics of this class of complexes are in progress.

Acknowledgment. Acknowledgment is made to the Petroleum Research Fund, administered by the American Chemical Society, for support of this research. D.J.B. is the recipient of a NSF Predoctoral Fellowship. We thank Melinda L. Greer and John M. Farrar for assistance with the electrochemical measurements. Funds for the X-ray diffraction facility at Vanderbilt University were provided through NSF Grant CHE-8908065.

Supporting Information Available: Listings of complete atom fractional coordinates and *B* values, bond distances and angles, and anisotropic thermal parameters (23 pages). Ordering information is given on any current masthead page.

OM960740+

(53) Sabbatini, M. M.; Cesarotti, E. *Inorg. Chim. Acta* **1977**, *24*, L9−L10.